

Regional representativity of AERONET observation sites in South America determined by correlation studies with MODIS Aerosol Optical Depth

Hoelzemann¹, Judith J., Karla M. Longo^{1,2}, Rafael M. Fonseca¹, Nilton M.
E. do Rosário³, Hendrik Elbern^{4,5}, and Saulo R. Freitas¹

submitted to JGR-Atmospheres

¹ CPTEC / INPE - Center for Weather Forecast and Climate Studies at the Brazilian National Institute for
Space Research, Cachoeira Paulista, São Paulo, Brazil

² now at DGE / INPE - Spatial Geophysics Division of the Brazilian National Institute for Space
Research, São José dos Campos, São Paulo, Brazil

³ IAG / USP - Institute of Astronomy, Geophysics and Atmospheric Science at the University of São
Paulo, São Paulo, Brazil

⁴ RIU - Rhenish Institute for Environmental Research at the University of Cologne, Cologne, Germany

⁵ now also at Institute for Chemistry and Dynamics of the Geosphere 2, Research Center Juelich,
Germany

Abstract

This paper presents an analysis of in-situ Aerosol Optical Depth (AOD) observations by
the AERONET network in South America from 2001-2007 in comparison with the
satellite AOD product of MODIS, aboard TERRA and AQUA satellites. Data of 12
observation sites were used with primary interest in AERONET sites located in or

downwind of areas with high biomass burning activity, and with measurements available for the full time range. Fires cause the predominant carbonaceous aerosol emission signal during the dry season in South America, and are therefore a special focus of this study. Interannual and seasonal behavior of the observed AOD at different observation sites were investigated, showing clear differences between purely fire and urban influenced sites. Correlations of AERONET and MODIS AOD, regarding TERRA and AQUA separately, revealed neither that neither an interannual trend may be observed nor that correlations differ significantly due to different overpass times. Individual anisotropic representativity areas for each AERONET site were derived by correlating AOD of each site for all years with available individual MODIS AOD pixels. The resulting climatological areas of common regional aerosols regimes often extend over several hundreds of kilometers, sometimes far across national boundaries. As a practical application, these strongly inhomogeneous and anisotropic areas of influence are being implemented in the tropospheric aerosol data assimilation system of CPTEC/INPE's CCATT-BRAMS model, promising an improved exploitation of information contents and thus, chemical weather forecast.

1. Introduction

Aerosols are one of the largest uncertainties of climate forcing. A better understanding of current climate change is still hampered by the prevalent insufficient knowledge on the impact of aerosols on solar radiation fluxes and the earth's albedo (Forster et al., 2007 (IPCC)). The direct radiative impact of aerosols is scattering and absorption of incoming solar radiation (e.g. Seinfeld and Pandis, 1998). The indirect impact refers to the interaction of aerosols with clouds. Aerosols can lead to variations in cloud microphysics, which in turn can impact cloud radiative properties and climate (e.g. Twomey (1977), Albrecht (1989), Kaufman (1995), Lohmann and Feichter (2005)).

The geographical, seasonal and inter-annual distribution, chemical composition, and properties of aerosols are in general highly variable. This is particularly true for smoke aerosols in the atmosphere over South America. Every year during the burning season, smoke particles released from biomass burning activities represent the major aerosol source. In the vicinity of mega-cities, urban-industrial emissions may be predominant however, on the continental scale sources are mainly composed of carbonaceous aerosol and trace gas emissions from deforestation and savanna maintenance fires. Hundreds of thousands vegetation fires, primarily in cerrado and forest ecosystems, emit vast amounts of aerosol particles into the atmosphere during the burning season (Setzer and Pereira (1991), Artaxo et al. (2005)). These fires occur mostly in the Amazonian region and Central Brazil, however, by atmospheric transport, their emissions produce a spatial smoke distribution over a large area of about 3-5 million km² (Artaxo et al., 2006). This is considerably higher than the area where the fires sources are concentrated (Freitas et al., (2005) and (2007a)). Aerosol effects by fires may go far beyond the local scale and significantly affect the hydrological cycle on a regional scale, including consequences in the redistribution pattern of tropical planetary energy to medium and high latitudes. If

1 meteorological conditions are favorable, the smoke plumes can be injected into altitudes
2 above the planetary boundary layer (e.g. Andreae et al. (2001), Freitas et al, (2007b)).
3 From there they can even be transported over thousands of kilometers on an
4 intercontinental scale. These smoke aerosols act as climate forcing (e.g. Kaufman and
5 Fraser (1997), Christopher et al. (2000)) and change chemical air composition. The
6 resulting smoke aerosol load often leads to heavy pollution and thus, to health effects on
7 the population.

8 Since some years, operational chemical weather forecasts are produced in many
9 countries to inform the population on critical levels of aerosol and trace gas
10 concentrations in the air. Mostly, these efforts are in conjunction with research and
11 development of chemical weather prediction models and case studies over longer
12 periods to understand and improve the underlying chemistry, vertical and horizontal
13 transport processes, emission sources, trends, and variabilities of tropospheric chemical
14 composition. However, there are several uncertainties inherent in these atmospheric
15 models due to unknown or not yet fully understood processes.

16 In the last decades, satellite aerosol products have become available to help reduce these
17 uncertainties on the tropospheric aerosol load (e.g. MODIS (Moderate Resolution
18 Imaging Spectroradiometer) aboard NASA's TERRA and AQUA satellites, MODIS-
19 like products from VIIRS (Visible Infrared Imaging Radiometer Suite), SeaWiFS (Sea-
20 viewing Wide Field-of-view Sensor), POES NOAA/AVHRR (Polar Operational
21 Environmental Satellite), TOMS (Total Ozone Mapping Spectrometer), CALIPSO
22 (Cloud-Aerosol Lidar and Infrared Pathfinder Satellite Observation) with vertical
23 resolution, or the European MSG-SEVIRI (Meteosat Second Generation - Spinning
24 Enhanced Visible and Infrared Imager, and other satellite platforms as GOME (Global
25 Ozone Monitoring Experiment), ATSR (Along-Track Scanning Radiometer) on board

1 of ERS2 (European Remote Sensing satellite 2), SCIAMACHY (Scanning Imaging
2 Absorption Spectrometer for Atmospheric CHartographY) and AATSR (Advanced
3 ATSR) on ENVISAT/ENVironmental SATellite). Satellite observations may detect
4 unknown global or regional patterns, daily variations and seasonalities that are not
5 reproduced by models. These data may be used to validate atmospheric models by
6 intercomparison efforts, or to directly improve model results by data assimilation
7 techniques. On the other hand, geographically sparse ground-based measurements exist,
8 with usually smaller errors. They play an important role to validate satellite data and
9 models however, the quantity of data is very small compared to satellites.

10 Successful air pollution modeling with the aim to reconstruct or predict a realistic
11 chemical state of the atmosphere requires good information on sources. The
12 atmospheric numerical model CCATT-BRAMS (Coupled Chemistry-Aerosol-Tracer
13 Transport model coupled to the Brazilian developments on the Regional Atmospheric
14 Modeling System (BRAMS)) (Walko et al., (2000), Freitas et al. (2005) and (2007a))
15 used at CPTEC / INPE makes use of the Brazilian Biomass Burning Emission Model
16 (3BEM) to provide daily fire emission estimates (Longo et al., 2007). Although making
17 best use of all available data, such as three different fire satellite products, emission
18 factors, burning efficiencies, and biomass loads from literature, considerable
19 uncertainties prevail in absolute emission fluxes.

20 One solution to correct these uncertainties may be the assimilation of aerosol satellite
21 data into CCATT-BRAMS. Before that, it is of utmost importance to assess the skill of
22 potential assimilation data to gain knowledge on improvements that may be expected by
23 assimilation. For assimilation purposes, focusing on South America, tropospheric
24 columns of satellite Aerosol Optical Depth derived from MODIS, collection 5 (C5), and
25 ground-based AOD observations from the AERosol RObotic NETwork (AERONET) are

1 available. MODIS satellite data exist on a daily, near-real-time operational basis,
2 starting in the year 2001 for TERRA satellite and 2002 for the MODIS instrument
3 aboard AQUA. Existing studies that have evaluated and intercompared these data
4 mostly rely on older MODIS collection 4 (C4) data, investigate only 1-2 years or only
5 one site, or focus on other continents (e.g. Chu et al., (2003), Hauser et al. (2005),
6 Tripathi et al. (2005), Kovacs et al. (2006), Li et al. (2007), Misra et al. (2008), and de
7 Almeida Castanho et al. (2008)).

8 In this paper we present the first long term study on MODIS C5 AOD and AERONET
9 AOD intercomparison for South America covering the whole suite of years 2001 -
10 2007. The aim of this study is to shed more light on interannual and seasonal variability,
11 if particular trends in correlations of these data can be observed, and how correlation of
12 these data may add information that is valuable for later aerosol data assimilation
13 purposes.

14 On one hand the MODIS AOD product yields some caveats over South America and a
15 number of other regions around the globe, related to the application of a global
16 algorithm. This algorithm assumes general, averaged, global aerosol models (Remer et
17 al., 2005). However, absorption and optical properties of smoke and urban/industrial
18 aerosols present significant variabilities associated with local or regional characteristics.
19 (Dubovik et al., 2002). Therefore AOD data users are required to exploit the available
20 ground-based measurements as best as possible in addition to the satellite data. On the
21 other hand ground based data may strongly profit from information achieved by the use
22 of satellite data: correlations may be used to define a radii or area of influence of each
23 in-situ observation to spread this sparse and valuable information spatially around each
24 site based on a sound statistic approach.

This paper is organized as follows: we describe the observational data used in this study in section 2. Section 3 exposes correlation studies of AOD from satellite and in-situ measurement sites and establishes an isotropic approach to determine radii of influence for each AERONET observation site. Since in reality high correlations may favor specific geographical directions due to local orography, preferential wind directions, etc., section 4 introduces a more sophisticated methodology to derive anisotropic areas of influence for each AERONET site. In section 5 we present AOD time series and histograms and present and discuss results from the isotropic radii of influence and the derived anisotropic areas. Final conclusions are drawn in section 6.

2. Data

2.1 AERONET data description

The AERONET (Aerosol RObotic NETwork) program is a federation of ground-based remote sensing aerosol networks established by NASA and LOA-PHOTONS (CNRS), expanded by collaborators. The program provides a long-term, continuous and readily accessible public domain database of aerosol optical, microphysical and radiative properties (<http://aeronet.gsfc.nasa.gov>). AERONET provides globally distributed observations of spectral columnar Aerosol Optical Depth (AOD) measured with Cimel Sun Photometers (Holben et al. 1998).

In this study we used cloud-screened level 1.5 AOD at 500nm (τ_{500}) processed with the version 2.0 algorithm, interpolated to 550 nm using the Angstrom coefficient (α) for 440-675 nm (Correia and Pires, 2006):

$$\tau_{550\text{nm}} = \tau_{500\text{nm}} / \exp[-\alpha \ln(\lambda_{500} / \lambda_{550})] \quad (1)$$

This interpolation guarantees comparability to the MODIS AOD at 550 nm. A filter developed by Pires et al. (2006) was applied to the level 1.5 AERONET data prior to comparison with MODIS data. The method makes use of regional Angstrom coefficient climatology to allow a more restrictive identification of cloud contaminated measurements. Data below a site-specific threshold of Angstrom coefficient from 440-675 nm are eliminated from the data base. By these means an additional amount of 2% - 13% of contaminated measurements are removed from the record (Pires et al., 2006). In the official AERONET level 2.0 data base up to 40% of measurements are eliminated from some site records, which possibly indicates an excess of applied thresholds. We experienced that the Pires et al. (2006) filtering method proofed to be as effective, while retaining most of the valuable and valid data.

Measurements of 12 South American sites were used in (**Figure 1**) with primary focus on sites with availability of the whole time series from 2001 – 2007 to ensure statistical significance. **Table 1** provides information on exact location and altitude of these 12 sites, as well as a categorization whether the site is located in a more rural or urban environment and if it is directly situated in a region with high fire occurrence (B) or if it is mainly influenced by transport of biomass burning emissions (BT). Sites that were main focus of this study with high undisturbed AOD at 550 nm (henceforth simply AOD) signals during fire season and with a full record of measurements from 2001 - 2007 are dark grey shaded. Urban sites presented in this study with a near to full record of measurements are light grey shaded. The seasonal mean AOD value calculated with all available data from August to September 2001 - 2007, separately at TERRA and AQUA over pass times (denoted "T" and "A", respectively), show a much higher AOD mean for AERONET sites located close to the fire emission sources than for urban

observation sites. Sites with high fire influence frequently yield maximum AOD values of up to 3, while urban sites mostly remain below 1. The standard deviations indicate a stronger AOD variation for all sites during the burning season.

2.2 MODIS data description

2.2.1 MODIS Level 2 Aerosol Optical Depth

The MODIS instrument aboard TERRA and AQUA satellites, that are part of the NASA-centered international Earth Observing System (EOS), delivers global retrievals of columnar Aerosol Optical Depth at 550 nm (AOD) since the year 2000 (TERRA and 2002 (AQUA). This study uses the Atmosphere Level 2, Collection 5 (C5) product (MOD04_02 and MYD04_02) from 2001-2007, described in the MODIS ATBD-MOD-02-document by Remer et al. (2006), available at: http://modis.gsfc.nasa.gov/data/atbd/atmos_atbd.php and Levy et al. (2007a and b). Data is available from the MODIS Adaptive Processing System (MODAPS) Services website (<https://modaps.nascom.nasa.gov:8499/>). The data are delivered in Hierarchical Data Format (HDF) for individual tiles with a resolution of 10 km x 10 km (at nadir) of each pixel. Overpass times of TERRA and AQUA over South America occur between 12 a.m. and 3 p.m. UTC, and from 4 p.m. to 7 p.m. UTC, respectively. **Figure 2** shows a typical AOD 550 nm scene monitored by TERRA during high biomass burning season over South America on September 3, 2005.

2.2.2 MODIS Level 3 gridded AOD from MOVAS

Gridded daily MODIS Level 3 collection 5 data (MOD08_D3.005 and MYD08_D3.005) separated for TERRA and AQUA at a spatial resolution of $1^\circ \times 1^\circ$ is available from the Giovanni MODIS Online Visualization and Analysis System (MOVAS) located at <http://daac.gsfc.nasa.gov/techlab/giovanni>. These MODIS data are used in the approach presented in section 4 for the years 2001 to 2007, where gridded data is required to provide full spatial coverage and computational efficiency.

3. Comparison of MODIS and AERONET Observations in South America

Daily and hourly means of AERONET AOD from 2001 – 2007 were compared with the corresponding TERRA/AQUA MODIS overpass. One MODIS pixel is equivalent to an area of about 10×10 km (at nadir). MODIS AOD was spatially averaged to be compared with AERONET in-situ AOD taking into account different radii around each AERONET site: a spatial mean was calculated for 1, 9, 25, and 225 MODIS pixels, respectively. This corresponds approximately to areas of 10×10 km, 30×30 km, 50×50 km, and 150×150 km around each site. AERONET AOD values were calculated as daily and hourly means, that is 30 minutes before MODIS overpass and 30 minutes after MODIS overpass. AQUA and TERRA data were processed separately because of their different overpass times and thus, different pollution scenarios over the continent. Smoke pollution during the burning season in Brazil shows a distinct peak during the afternoon (maximum ~3p.m. local time) close to AQUA overpass, while TERRA crosses the Southern American continent during the morning. Correlations were calculated for all AERONET stations with available data for at least 3 years of the

period 2001-2007 (**Table 1**). As expected correlation is higher for AERONET hourly mean AOD for all MODIS samples and were therefore used throughout this study.

The main objectives were to identify systematic differences in correlations of TERRA and AQUA AOD data, explore if a trend exists in the data within the interannual variability, and to investigate whether the correlation studies with the spatial means of MODIS data around each AERONET site may serve to establish radii of influence as additional background information for tropospheric aerosol data assimilation purposes. As in-situ observation sites are rare and sparsely located with several hundred of kilometers distance, it is important to make optimal use of available information at the sites. Introducing validated radii of influence (or decorrelation lengths) a region around each AERONET site can be determined by statistical means that may profit from the retrieved AOD at the site during assimilation.

4. Regional Anisotropic Representativity Studies: Methodology

The quest up to which distance from a measurement site observational information can be used to analyze atmospheric fields and initial data provision is a key challenge for efficient data assimilation. Typically, pairwise correlation calculations of stations serve as the basis for the identification of radii of influence (or decorrelation lengths), where no specification is made with respect to individual dependence of station locations and characteristics (homogeneity assumption) and uniform correlation lengths for each direction is assumed (isotropy assumption).

With the advent of satellite data, the data bases are significantly extended and this richness can be used to identify detailed areas of representativity. From a technical viewpoint, in data assimilation parlance, anisotropic areas of influence or decorrelation

lengths can be designated. The anisotropic definition of a radius of influence is more appropriate as it may better represent natural conditions of some similarity around an observation site. Moreover, a term like “area of influence“ is better suited to denote prevailing similarity conditions (see Elbern et al. (2007) for a practical way to handle related covariance matrices in data assimilation). As a consequence, in addition to the isotropic approach for introduction of radii of influence for each AERONET site in section 3, an anisotropic statistical approach was developed taking into regard climatological AOD information.

The method chosen for creating anisotropic radii of influence for each of the 12 South American AERONET sites relies on a correlation study of AERONET and $1^\circ \times 1^\circ$ gridded MODIS AOD data (MOVAS, see section 2.2.2) for the burning seasons from 2001 - 2007 (i.e. August 1st to October 31st). For the present approach the gridded MODIS data was preferred to the original ungridded 10 km x 10 km pixels (see section 2.1.2) to guarantee full spatial coverage and efficient computability, which is a prerequisite for its application in a data assimilation code.

A Pearson correlation map was calculated for each AERONET site with regard to all MOVAS AOD grid boxes (correlation at grid box with indices i and j for a specific site: $\text{Corr}_{\text{site}}(i,j)$) for the complete burning season record from 2001 - 2007:

$$\text{Corr}_{\text{site}}(i, j) = \text{Corr}[\tau_{\text{aero}}(x, y, t), \tau_{\text{movas}}(i, j, t)], \quad \forall t \in [1/8/2001, 31/10/2007] \quad (2)$$

where τ_{aero} , τ_{movas} are the respective AOD's, x,y are the coordinates of a specific AERONET site, i,j , are the indices of all $1^\circ \times 1^\circ$ gridded MOVAS grid points, and t is the time. These maps are presented in **Figure 10** and shall be discussed in section 5.3.

To gain an overview of extent and limits of influence of each AERONET site the areas of influence needed to be aggregated into a single consistent map. In practice the gained climatological information on regional correlation of each AERONET site can be applied for formulation of the background error covariance matrix. Thus, an array was computed by identifying the site with the highest correlation for each $1^\circ \times 1^\circ$ grid box (**Figure 11**). This part of the study was also distinguished between TERRA and AQUA AOD products to investigate a possible different behavior due to differing overpass times. In this final dominant influence map, only values of $R^2 > 0.5$ were considered as appropriate to define a sustained area of influence around each site. Favoring a conservative approach, spurious pixels that identify disconnected and often remote spots of high AERONET / MODIS correlations of a site were also eliminated from the map.

5. Results and Discussion

5.1 Interannual and seasonal AOD variation

Figure 3-5 present hourly mean AOD 550nm records by AERONET (in red, taken at MODIS over pass time), and MODIS (black) aboard TERRA and AQUA from 2001 – 2007, located over AERONET observation sites. Data from TERRA yields the longest time series starting in 2001 (**Figure 3**). This figure shows the four AERONET observation sites with records over the observed period and predominant signals from biomass burning emissions (see also **Table 1**): Abracos Hill, Rio Branco, Cuiabá-

Miranda and Alta Floresta, all located in Brazil in areas with high fire activity. The AOD regularly peaks during the burning season from August to October for all measurement sites. Highest AOD was observed for the year 2007 at all sites. 2001, 2003, and 2004 were years with lower AOD signal, due to a lesser occurrence of fires. Generally, MODIS AOD reaches a higher maximum AOD than measurements from AERONET, while it underestimates low AOD values compared to the in-situ observations. Li et al. (2007) conducted a study in China comparing AOD of the MODIS C4 and C5 algorithm with in-situ Sun photometer observations and attributed the discrepancies to the choice of aerosol type in the algorithm's aerosol model. In the MODIS C5 data suite, the aerosol models are modified according to AERONET observations. These are possibly taken under conditions with very different emission scenarios and thus induce regional biases into the data when applying it to regions with very different situations, such as China (Li et al. 2007), or Brazil. Kinne et al. (2003) suggest that the MODIS AOD high-bias may be explained to the fact that AERONET sites only measure AOD under cloud-free conditions, whereas MODIS is able to detect aerosols under more cloudy patterns, often associated with higher AOD levels. Further studies report MODIS AOD overestimates such as Ichoku et al. (2005), Abdou et al. (2005), and Hauser et al. (2005).

Figure 4 presents the same site's records for MODIS/AQUA, launched in May 2002, with the respective AERONET AOD hourly mean taken at the satellite's overpass time in the afternoon. Visibly, AQUA observations are less dense than for TERRA for all years and observation sites, which can be attributed to general higher cloud coverage in the afternoon (AQUA) than during the morning (TERRA) (Koren et al., 2004).

Other AERONET sites influenced by South American biomass burning activity are Campo Grande in the Brazilian state Mato Grosso do Sul and Santa Cruz in Bolivia (not

1 shown). Despite their vicinity to urban infrastructure and thus exposure to industrial and
2 vehicular emission sources, these sites yield a clear and significant signal of elevated
3 AOD due to transported and local biomass burning emissions during the burning
4 season.

5 An example of AERONET sites with clearly urban properties is shown in **Figure 5**. The
6 sites in São Paulo and in Buenos Aires (CEILAP-BA) show a more diffuse AOD
7 pattern than those sites exposed mainly to biomass burning emissions. São Paulo
8 however, also yields an elevated AOD signal during austral winter. These maxima are
9 related to lower precipitation rates and the typical more stable Planetary Boundary
10 Layer (PBL) during this period, nevertheless, most extreme events are indeed associated
11 with biomass burning emission transport from deforestation and maintenance fires in
12 other Brazilian states such as Mato Grosso do Sul, Mato Grosso, Rondônia, and Acre.
13 Also inside the state of São Paulo carbonaceous aerosols may be emitted from
14 agricultural motivated fires and fires related to sugar cane harvesting during the dry
15 season from June to October. In this season atmospheric blocking events may occur,
16 leading to stagnating weather conditions that favor an accumulation of aerosols over
17 São Paulo, and thus enhanced tropospheric AOD.

18 In Buenos Aires the impact from fires on the tropospheric aerosol load is less visible
19 however, it is known that the fire plumes from Central Brazil are often transported over
20 Argentina (Freitas et al., 2007). Agricultural fires in the floodplain of the Paraná River
21 northwest from Buenos Aires, may carry intense fire-plumes over the city, such as
22 recently documented by Faries and Raszewski (2008) and visible on MODIS fire
23 product images (<http://earthobservatory.nasa.gov/NaturalHazards/>) on April 17, 2008.
24 Elevated AOD measurements, as shown in **Figure 5** may thus be either related to large

scale fire emission transport from Central Brazil, or from regional transport from national territory.

The other urban AERONET sites in South America with measurements from 2001-2007 are Córdoba-CETT, also in Argentina, and Santiago in Chile (not shown). For the latter only a very short period of AOD data was measured by AERONET (parts of 2001 - 2002). and MODIS AOD yields a signal that cannot yet be fully explained but seems to be related to an inappropriate assumption on vertical aerosol distributions and treatment of cirrus clouds (Oyanadel et al., (2006) and L. Gallardo, pers. communication. (2008)). Córdoba however, shows a seasonal behavior with elevated AOD during the South American burning season that may be associated to the transport of fire emissions from the north/northwest, as well as local fire activity. Generally, AOD at urban sites has systematically lower maxima than those sites located in or under impact of fire active regions and seldom exceed an AOD of 1.

Finally, the AERONET site Belterra, located in the north of Brazil, a rural site and remote from fire activity, shows a burning season related AOD variability due to transport of fire emissions with AOD regularly below 0.6. The AOD record of Petrolina, further to the northeast, was investigated for similar transport features. Only few AERONET measurements were carried out at this site, according to MODIS a seasonal variability seems to exist with a varying maximum AOD below 0.3 between September and December, which may be related to fires.

Table 1 provides absolute values of seasonal mean AERONET AOD, its standard deviation, and absolute AOD maxima separately for TERRA and AQUA overpass time throughout all seven burning seasons from 2001-2007. A large difference of maximum AOD values can be observed for sites in or close to regions with high biomass burning activity. The highest AOD (4.7) is observed during an afternoon overpass by AQUA at

Cuiabá Miranda. Generally, standard deviations are high, in the order of the mean values, which indicate the high variability of AOD during the biomass burning seasons. The sites Cuiabá Miranda, Rio Branco and Campo Grande yield higher mean and maximum AOD's during AQUA afternoon overpass, which coincides with the 3 p.m. (local time) maximum of burning activity. At other sites influenced by fire plumes AQUA time AOD is similar or inferior to that of TERRA overpass time. This may be related to the much higher omission in observations due to regular higher cloud coverage during the afternoon. Another superposing effect may be that the aerosol dispersion and removal processes are generally more intense about noon, after TERRA and before AQUA overpass: during the morning aerosol plumes stick close to the surface due to reduced convection over night and the reduced height of the planetary boundary layer. This effect results in slow dispersion in the atmosphere and may thus lead to differences in observed TERRA (morning) and AQUA (afternoon) mean and maximum AOD.

Urban sites yield a considerable lower mean (<0.5) and maximum AOD (<1.8). The AERONET site located in São Paulo also shows a higher seasonal mean AOD during AQUA overpass time, which may also be related to transport of biomass burning emissions over the city, coming from other states, or from sugar cane burning activities in the state of São Paulo.

To demonstrate the occurrence of high AOD and typical distributions at each AERONET site we present six AOD bins as histograms, comprising all available years of data (**Figure 6**). Results are presented for hourly mean AERONET AOD at TERRA overpass time during morning, and were compared to those measured during AQUA overpass (not shown). Since the histograms are very similar and the TERRA time AOD yields more data points and the whole suite of years, only AOD at TERRA overpass is

presented. Alta Floresta, Rio Branco and Cuiabá-Miranda, the biomass burning influenced sites, show high AOD's for the years 2005-2007, and to a somewhat lesser extent, also for 2002 (Alta Floresta). Most AOD data points are however located in the AOD range from 0.3 – 0.6, followed by the AOD bin 0.6-1.0. The urban AERONET sites, such as São Paulo and Buenos Aires (CEILAP-BA), only observed AOD's with values in the < 0.3 range and with few values in the 0.3-0.6 bin.

5.2 Isotropic representativity of AERONET sites

Figures 7 - 9 present the results of the isotropic, spatial correlation study described in section 3. We have chosen the AERONET site of Alta Floresta as a typical example how correlations behave during the burning seasons (August to October) from 2001 - 2007. In **Figure 7a** correlations are presented for MODIS/TERRA and correspondent AERONET hourly mean AOD. Generally, it can be observed that: (i) R^2 correlations are high (> 0.7), (ii) as linear regression yields a slope > 1 MODIS tends to overestimate AOD, except for low values, and (iii) no apparent interannual trend of correlation or slope can be found from 2001 - 2007. Especially at the site Alta Floresta it was expected that the strong land cover change occurring in the vicinity of this site, associated to deforestation processes and thus, fire activity, could provoke a trend in correlation patterns along the years: The forest line, and thus the region of deforestation activity, is continuously receding from Alta Floresta, which might be visible in in-situ measurements of AOD, but not on a low resolution remote sensing AOD product. Since no trend could be observed for any of the sites, the latter item (iii) suggests a compilation of all years data to provide a more solid statistical basis by augmenting the

number of record elements (N), as shown in the bottom right panels of **Figures 7 a and b** for Alta Floresta. Properties (i - iii) prevail for all AERONET sites subject to biomass burning emissions, and thus elevated AOD during the burning season. The patterns are repeated in the correlation study with MODIS/AQUA AOD (**Figure 7b**). AOD correlation based on all years (2001 -2007) of other AERONET sites are shown in **Figure 8**. The patterns (i) to (ii) are the same as for Alta Floresta, except for the urban sites with an AOD < 1. The threshold in (ii), where the systematic bias between AERONET and MODIS AOD is inverted, varies between an AOD of 0.3 and 0.7.

These correlation results are in contrast to the global validation of the MODIS AOD C3 and C4 product by Remer et al. (2005). A corresponding global correlation figure for data points over land presents a positive MODIS for small AOD's and an underprediction for high values. Since these results are based on global data and for the period 2000-2002 it is most certain not representative for specific conditions in South America. Further, the MODIS C4 algorithm validated in Remer et al. (2005) employs a nondust, moderate absorption aerosol model (applied to regions under influence of forest smoke and urban emissions in developing countries) in South America. This aerosol model uses a single scattering albedo $\omega_o(550\text{ nm}) = 0.90$ for the whole year and continent. The optical aerosol property ω_o determines the sign of radiative forcing, i.e. cooling or heating, (Hansen et al., 1997) and is thus crucial for a correct representation of the aerosol load in the atmosphere. AERONET ground retrievals presented in the work of Dubovik et al. (2002) yield a higher ω_o at 550 nm for Amazonian forest (0.94) and a lower for Brazilian Cerrado (0.90). Other in-situ measurements reported in Dubovik et al. (2002) present lower numbers, such as $\omega_o = 0.86$ for Amazonian forest, $\omega_o = 0.79$ (local smoke) and $\omega_o = 0.85$ (aged smoke) for Cerrado (Reid et al., 1998).

1 These differences in the single scattering albedo may significantly change aerosol load
2 calculations.

3 The MODIS C5 AOD product used in this study makes use of updated aerosol model
4 look up tables (LUT's). Levy et al. (2007a) performed a subjective seasonal cluster
5 analysis with AERONET data to produce new LUT's with more realistic regional
6 optical properties. The region of southern Central Brazil and the southeastern region of
7 Brazil is now attributed to the highly absorbing aerosol model from June to November
8 with $\omega_0 = 0.85$, formerly only applied to Southern Africa. During the remaining year
9 and other parts of the Southern American continent, the moderately absorbing aerosol
10 model is assumed with $\omega_0 = 0.90$, such as in the earlier C4 version. The cluster analysis
11 chooses the predominant fraction of the assigned aerosol model to each AERONET
12 observation separately for the seasons DJF, MAM, JJA, and SON. The main burning
13 season in Central Brazil takes place from August to September. Possibly, both the
14 seasons JJA and SON defined in the study include a number of AERONET
15 measurements before the onset and after the offset of the burning season, thus finding a
16 high percentage of moderately absorbing aerosol, which may lead to a non-
17 representative attribution of optical aerosol properties to the observation sites located in
18 northeastern Central Brazil.

19
20 To derive isotropic radii of influence from the present correlation study we investigated
21 how the correlation behave when expanding the MODIS area and using different sizes
22 of spatial averages of MODIS AOD around each AERONET site, as described in
23 section 3. Results of this approach are depicted in **Figure 9** for the site Rio Branco,
24 located in the state Acre of northwestern Brazil. In the panels (a) to (d) the spatial area
25 where MODIS AOD is averaged is increased from 10 km x 10 km (1 MODIS pixel), 30

1 km x 30 km (9 pixels), 50 km x 50 km (25 pixels), to 150 km x 150 km (225 pixels).
2 This spatial MODIS AOD average is then correlated with the site's AERONET AOD.
3 Rio Branco is highly affected by fires during the burning season. These fires occur
4 mostly in the Amazonian region and Central Brazil, however, by atmospheric transport,
5 their emissions produce a spatial smoke distribution over a large area of about 3-5
6 million km² (Artaxo et al., 2006). This is considerably higher than the area where the
7 fires sources are concentrated (Freitas et al. (2005) and (2007a)). Therefore, spatial
8 correlations remain very high, even when applying an AOD value, spatially averaged
9 over a very large area of 150 km x 150 km, to calculate AOD correlations. In fact, the
10 larger the averaged area, the stronger the tendency that the linear regression slope goes
11 towards the value 1. The same is true for all other sites that are located in this fire-
12 impacted region. On one side this means that a large radius of influence may be suitable
13 for these sites. However, the isotropy of this approach possibly ignores that various sub-
14 regions within the reach of this radius may inhere a different scenario, and thus infers a
15 representativity error. One possibility would be to refine this isotropic approach, such as
16 Kovacs (2006), who calculated correlations of equidistant pixels around a site.
17 In his study we have opted for an anisotropic approach (next section) that will be able to
18 provide a preferential treatment to geographical directions that yield higher correlations.
19 Derived from a sound statistical basis, these areas of influence will be more adequate
20 for later data assimilation purposes.

5.3 Anisotropic representativity of AERONET sites

A more sophisticated approach than isotropic influence radii is the use of more realistic anisotropic areas of influence for each AERONET site, calculated according to the methodology in section 4.

The resulting AOD correlation arrays over South America for each AERONET site with regard to all MOVAS TERRA (top) and AQUA (bottom) AOD grid boxes for the burning seasons from 2001 - 2007 are shown in **Figure 10**. The AERONET sites Belterra, Santiago and Petrolina were excluded from this step as a solid amount of data is missing to support reliable statistics and these sites are not located in the main region of interest with high impact of biomass burning activity. Most sites present strongly anisotropic and inhomogeneous shape of area with moderate to strong AOD correlations with MOVAS. Rio Branco, Santa Cruz, and Campo Grande yield the largest areas of influence, spreading over several state and country borders. A noticeable pattern is the northwestern transport of biomass burning emission loaded air and, to a lesser extent, also towards the southeastern direction, especially notable for Santa Cruz and Campo Grande. The sites Abracos Hill, Alta Floresta and Cuiabá-Miranda show smaller and more isotropic radii of influence, but the correlation clearly show that observations from these sites may be used to exploit the measurements for much larger areas for assimilation based chemical state analyses and model initialization. The appearance of the obtained areas of influence can be explained with climatological meteorological patterns over South America: generally, during the dry season, Central Brazil is dominated by a high pressure area with low precipitation and light winds in the lower troposphere (Satyamurty et al., 1998). Convection in the Amazon basin is shifted to the northwestern part of South America. These conditions are associated with the westward displacement of the South Atlantic Subtropical High (SASH) and the northward motion

of the Intertropical Convergence Zone (ITCZ) during the austral winter. The position of the SASH determines the inflow of clean maritime air into the biomass burning area, playing an important role in defining the shape of regional smoke plumes, as the SASH is the primary mechanism responsible for dilution of polluted air. Approaching cold frontal systems from the south are responsible for disturbances in atmospheric stability and in the wind field. These changes define the main corridors of smoke export to oceanic areas. The Andes Mountains on the east side of South America, together with the SASH, impose a long range transport of smoke from its source areas to the South and Southeast of the South American continent, thus disturbing larger areas downwind in the subtropics. The two major areas of inflow and outflow are north of the Equator with the inflow of smoke from African fires and a smoke outflow from SA fires to the Southern Atlantic Ocean and to the African continent (Freitas et al., 2007).

In **Figure 11** the individual correlations obtained in **Figure 10** were compiled to a single map with dominant influence areas for each site. Each color of **Figure 11** represents the radius of influence of a specific site, denominated in the figure's legend and in the legend of Figure 10. The radii of influence were restricted to correlations of $R^2 > 0.5$. In addition, a conservative approach has been chosen that fulfills a continuity criterion: the areas of influence may remain contingent, thus only connected grid points starting from the site's location are considered. Spurious grid points with high correlations were excluded from the final map.

TERRA results (a) generally yield similar patterns as those from AQUA (b), with some differences in detail: the AQUA influence area of Santa Cruz and Rio Branco do not extent as far into northern Peru as with TERRA, the influence areas for Abracos Hill and Cuiabá-Miranda are smaller, and Buenos Aires AOD's yields correlations $R^2 > 0.5$ and thus a notable correlation length.

1 In summary, **Figure 11** shows that in spite of the sparseness of in-situ measurement
2 sites, a significant area of South America may be characterized by AERONET AOD
3 observations.

4 5 6 7 **6. Conclusions**

8
9 In this paper we present an intercomparison study of MODIS satellite and in-situ AOD
10 observations in South America over the years 2001-2007, with special focus on
11 observations sites with a strong influence of fire emissions during the biomass burning
12 season. The objectives were to investigate possible trends of the time series, differences
13 between TERRA and AQUA MODIS AOD, and to establish regional representativity
14 criteria for the South American AERONET sites that may be used for AOD assimilation
15 into a Chemistry Transport Model.

16 Generally, all biomass burning influenced sites show a distinct augmentation in AOD
17 during the burning seasons of all years (August – October) with a maximum in
18 September. AOD at urban sites is considerably lower than at the fire influenced sites.
19 These features are equally well represented by AERONET and MODIS satellite data.
20 The correlation study, carried out separately for TERRA and AQUA data, revealed that
21 AERONET and MODIS data correlate generally well ($R^2 > 0.7$), with a slope bigger
22 than 1. MODIS data over South America yield a systematic bias: AOD is too low for
23 small AOD values and yields a high bias for elevated AOD's. For later data assimilation
24 purposes these systematic biases can be corrected during assimilation. No interannual
25 trend of correlation or slope could be found during the investigated period. Statistically,

1 no large differences could be observed between MODIS/TERRA and MODIS/AQUA
2 data. However, it will be useful to allow a separate assimilation into a model, to make
3 use of the temporal resolution, given by the two different overpass times.

4 The isotropic radii of influence derived for each AERONET site allow a spatial
5 distribution of observation validity over the model domain. However, they need to be
6 used with caution to not infer gross errors of representativeness. The more sophisticated
7 anisotropic approach provided strongly inhomogeneous and anisotropic areas of
8 influence based on AOD data for the burning seasons from 2001-2007. These
9 climatological influence areas cover large regions of the continent for some sites, which
10 in the future may have transboundary implications related to emission transport.

11 An influence map was derived for all observation sites that may directly be used by
12 AOD assimilation schemes, whose background error covariance matrix is prepared to
13 deal with anisotropic areas of influence. Such systems will highly profit from these
14 newly defined parameters, by distributing assimilated information on AERONET AOD
15 to neighboring grid points, based on sound statistics. The influence maps developed
16 during the present study will be used with the CCATT-BRAMS model at CPTEC/INPE.

17 The additional assimilation of AERONET AOD using these newly derived areas of
18 influence is expected to strongly contribute to an improvement of the model skill.

19 The anisotropic areas of influence map further pinpoints regions where additional AOD
20 measurement sites are needed to allow for a more complete observation coverage of the
21 South American continent. Beyond these technical aspects, they also indicate areas of
22 common aerosol chemistry regimes and their related geographical environmental
23 impact.

24 Our correlation study of MODIS versus AERONET AOD reaffirmed the importance of
25 a regional MODIS algorithm for AOD retrieval over South America with adequate

optical aerosol models. Pioneering work on this topic has been contributed by Correia (2006) and Correia et al. (2006) over biomass burning smoke influenced areas and by de Almeida Castanho et al. (2008) over the mega-city São Paulo. For aerosol data assimilation in South America it would be fundamental that this work be continued until achieving an operational status.

Acknowledgements:

Judith Hoelzemann is funded by the Brazilian "Fundação de Amparo à Pesquisa do Estado de São Paulo" (FAPESP) under grant 05/60890-3. We thank the AERONET Principal Investigators Brent Holben, Paulo Artaxo, and Enio B. Pereira and their staff for establishing and maintaining the 12 South American sites used in this investigation. We thank the NASA/MODAPS team for providing the whole suite of MODIS collection 5 data, and the NASA/MOVAS/Giovanni team at GES DISC for provision of gridded MODIS data.

References:

- Abdou, W. A., D. J. Diner, J. V. Martonchick, C. J. Bruegge, R. A. Kahn, B. J. Gaitley, and K. A. Crean (2005), Comparison of coincident Multiangle Imaging Spectroradiometer and Moderate Resolution Imaging Spectroradiometer aerosol optical depths over land and ocean scenes containing Aerosol Robotic Network sites, *J. Geophys. Res.*, 110, D10S07, doi:10.1029/2004JD004693.
- Albrecht, B. A. (1989), Aerosols, Cloud Microphysics, and Fractional Cloudiness, *Science*, Vol. 245. no. 4923, pp. 1227 - 1230, DOI: 10.1126/science.245.4923.1227.
- Andreae, M., Artaxo, P., Fischer, H., Freitas, S., Grégoire, J.-M., Hansel, A., Hoor, P., Kormann, R., Krejci, R., Lange, L., Lelieveld, J., Lindinger, W., Longo, K., Peters, W., Reus, M., Scheeren, B., Silva Dias, M. A. F., Ström, J., Velthoven, P. F. J. And J. Williams (2001), Transport of biomass burning smoke to the upper troposphere by deep convection in the equatorial region, *Geophys. Res. Lett.* 28 (6), 951.
- Artaxo, P., V. G. Gatti, A. M. C. Leal, K. M. Longo, S. R. de Freitas, L. L. Lara, T. M. Pauliquevis, A. S. Procópio, and L. V. Rizzo (2005), Química atmosférica na Amazônia: A floresta e as emissões de queimadas controlando a composição da atmosfera amazônica, *Acta Amazonica*, Vol. 35(2), p. 191-208.
- Artaxo, P., Oliveira, P.H., Lara, L.L.; Pauliquevis, T.M., Rizzo, L.V.; Pires, C., Paixão, M.A.; Longo, K.M.; Freitas, S.; Correia, A.L. (2006), Efeitos climáticos de partículas de

aerossóis biogênicos e emitidos em queimadas na Amazônia. Revista Brasileira de Meteorologia. , v. 21, n. 3, p. 168-189.

Christopher, S.A., J. Chou, J. Zhang, X. Li and R.M. Welch (2000), Shortwave Direct Radiative Forcing of Biomass Burning Aerosols Estimated From VIRS and CERES, Geophys. Res. Letters, vol. 27, pp. 2197-2200.

Chu, D. A., Y. J. Kaufman, G. Zibordi, J. D. Chern, J. Mao, C. Li, and B. N. Holben (2003), Global monitoring of air pollution over land from the Earth Observing System-Terra Moderate Resolution Imaging Spectroradiometer (MODIS), *J. Geophys. Res.*, 108(D21), 4661, doi:10.1029/2002JD003179.

Correia, A. L., Monitoring aerosol optical depth using MODIS over Brazil and South America (2006), In: Congresso Brasileiro de Meteorologia, 2006, Florianópolis. Anais do Congresso Brasileiro de Meteorologia, v. 1. p. 1-8.

Correia, A. L. and Pires Junior, C. A. (2006), Validation of aerosol optical depth retrievals by remote sensing over Brazil and South America using MODIS. In: Congresso Brasileiro de Meteorologia, 2006, Florianópolis. Anais do Congresso Brasileiro de Meteorologia, Vol. 1. p. 1-8.

Correia, A. L., Castanho, A. D., Martins, J.V., Longo, K.M., Yamasoe, M.A., Artaxo, P. (2006), Inferência de Aerossóis In: O sensor MODIS e suas aplicações ambientais no Brasil. ed. Bookimage, p. 297-314.

- 1 Dubovik, O., Holben, B. N., Eck, T. F., Smirnov, A., Kaufman, Y. J., King, M. D.,
2 Tanre, D., and Slutsker, I. (2002), Variability of absorption and optical properties of key
3 aerosol types observed in worldwide locations, *J. Atmos. Sci.*, 59, 590–608.
4
- 5 de Almeida Castanho, A. D., J. Vanderlei Martins, and P. Artaxo (2008), MODIS
6 Aerosol Optical Depth Retrievals with high spatial resolution over an Urban Area using
7 the Critical Reflectance, *J. Geophys. Res.*, 113, D02201, doi:10.1029/2007JD008751.
8
- 9 Elbern, H., A. Strunk, H. Schmidt, and O. Talagrand, (2007), Emission rate and
10 chemical state estimation by 4-dimensional variational inversion, *Atmos. Chem. Phys.*,
11 3749-3769.
12
- 13 Faries, B., and Raszewski, E. (2008), Smoke Cloaks Buenos Aires City as Farmers
14 Burn Fields. *Bloomberg.com*, April 17.
15
- 16 Forster, P., V. Ramaswamy, P. Artaxo, T. Berntsen, R. Betts, D.W. Fahey, J. Haywood,
17 J. Lean, D.C. Lowe, G. Myhre, J. Nganga, R. Prinn, G. Raga, M. Schulz and R. Van
18 Dorland (2007), Changes in Atmospheric Constituents and in Radiative Forcing. In:
19 Climate Change 2007: The Physical Science Basis. Contribution of Working Group I to
20 the Fourth Assessment Report of the Intergovernmental Panel on Climate Change
21 [Solomon, S., D. Qin, M. Manning, Z. Chen, M. Marquis, K.B. Averyt, M.Tignor and
22 H.L. Miller (eds.)]. Cambridge University Press, Cambridge, United Kingdom and New
23 York, NY, USA.
24

- 1 Freitas, S., K. Longo, M. A. F. Silva Dias, P. L. Silva Dias, R. Chatfield, E. Prins, P.
- 2 Artaxo, G. Grell, and F. Recuero (2005), Monitoring the transport of biomass burning
- 3 emissions in South America, *Environmental Fluid Mechanics*, 5, p. 135-167, 5th RAMS
- 4 Users Workshop Special Issue.
- 5
- 6 Freitas, S. R., K. M. Longo, R. Chatfield, D. Latham, M. A. F. Silva Dias, M. O.
- 7 Andreae, E. Prins, J. C. Santos, R. Gielow and J. A. Carvalho Jr. (2007a), Including the
- 8 sub-grid scale plume rise of vegetation fires in low resolution atmospheric transport
- 9 models. *Atmospheric Chemistry and Physics*, v. 7, p. 3385-3398.
- 10
- 11 Freitas, S. R., K. Longo, M. Dias, R. Chatfield, P. Dias, P. Artaxo, M. Andreae, G.
- 12 Grell, L. Rodrigues, A. Fazenda and J. Panetta (2007b), The Coupled Aerosol and
- 13 Tracer Transport model to the Brazilian developments on the Regional Atmospheric
- 14 Modeling System (CATT-BRAMS). Part 1: Model description and evaluation. *Atmos.*
- 15 *Chem. Phys. Discuss.*, 7., 8525-8569.
- 16
- 17 Hansen, J., M. Sato, and R. Ruedy (1997), Radiative forcing and climate response. *J.*
- 18 *Geophys. Res.*, 102, 6831-6864.
- 19
- 20 Hauser, A., D. Oesch, and N. Foppa (2005), Aerosol optical depth over land:
- 21 Comparing AERONET, AVHRR and MODIS, *Geophys. Res. Lett.*, 32, L17816,
- 22 doi:10.1029/2005GL023579.
- 23
- 24 Holben, B. N., T.F. Eck, I. Slutsker, D. Tanré, P.J. Buis, A. Setzer, E. Vermote, J.A.
- 25 Reagan, Y.J. Kaufman, T. Nakajima, F. Lavenue, I. Jankowiak and A. Smirnov (1998),

AERONET a federated instrument network and data archive for aerosol
characterization. Remote Sensing of Environment 66, pp. 116.

Ichoku, C., L. A. Remer, and T. F. Eck (2005), Quantitative evaluation and
intercomparison of morning and afternoon Moderate Resolution Imaging
Spectroradiometer (MODIS) aerosol measurements from Terra and Aqua, J. Geophys.
Res., 110, D10S03, doi:10.1029/2004JD004987.

Kaufman, Y. (1995), Remote sensing of direct and indirect aerosol forcing, in Aerosol
Forcing of Climate, ed. by R. J. Charlson and J. Heintzenberg, pp. 297-332, John Wiley,
New York.

Kaufman, Y. J., and R. S. Fraser (1997), The Effect of Smoke Particles on Clouds and
Climate Forcing, Science, vol. 277, pp. 1636-1639.

Koren, I., Y. J. Kaufman, L. A. Remer, J. V. Martins (2004), Measurement of the Effect
of Amazon Smoke on Inhibition of Cloud Formation, Science, 303 (5662), pp. 1342 -
1345.

Kovacs, T. (2006), Comparing MODIS and AERONET aerosol optical depth at varying
separation distances to assess ground-based validation strategies for spaceborne lidar, J.
Geophys. Res., 111, D24203, doi:10.1029/2006JD007349.

1 Levy, R. C., L. A. Remer, and O. Dubovik (2007a), Global aerosol optical properties
2 and application to Moderate Resolution Imaging Spectroradiometer aerosol retrieval
3 over land, *J. Geophys. Res.*, 112, D13210, doi:10.1029/2006JD007815.

4
5 Levy, R. C., L. A. Remer, S. Mattoo, E. F. Vermote, and Y. J. Kaufman (2007b),
6 Second-generation operational algorithm: Retrieval of aerosol properties over land from
7 inversion of Moderate Resolution Imaging Spectroradiometer spectral reflectance, *J.*
8 *Geophys. Res.*, 112, D13211, doi:10.1029/2006JD007811.

9
10 Li, Z., F. Niu, K.-H. Lee, J. Xin, W.-M. Hao, B. Nordgren, Y. Wang, and P. Wang
11 (2007), Validation and understanding of Moderate Resolution Imaging
12 Spectroradiometer aerosol products (C5) using ground-based measurements from the
13 handheld Sun photometer network in China, *J. Geophys. Res.*, 112, D22S07,
14 doi:10.1029/2007JD008479.

15
16 Lohmann U., Feichter J. (2005), Global indirect aerosol effects: a review, *Atmos.*
17 *Chem. Phys.*, 5, p. 715-737.

18
19 Longo, K., S. R Freitas, A. Setzer, E. Prins, P. Artaxo, and M. Andreae (2007), The
20 Coupled Aerosol and Tracer Transport model to the Brazilian developments on the
21 Regional Atmospheric Modeling System (CATT-BRAMS). Part 2: Model sensitivity to
22 the biomass burning inventories. *Atmos. Chem. Phys. Discuss.*, 8571-8595.

Misra, A., A. Jayaraman, and D. Ganguly (2008), Validation of MODIS derived aerosol optical depth over Western India, *J. Geophys. Res.*, 113, D04203, doi:10.1029/2007JD009075.

Oyanadel, A., Painemal, D., Léon, J-F, Chiapello, I., Gallardo, L. (2006), Aerosol loading over Santiago de Chile: a comparison between satellite and in-situ measurements, *Proceedings of the 8th International Conference on Southern Hemisphere Meteorology and Oceanography (8 ICSHMO)*, Foz do Iguaçu, Brazil, April 24-28, 2006, INPE, p. 149-155.

Pires, C., A. Correia, M. A. Paixo, e P. Artaxo, (2006), Estudo da climatologia regional de coeficiente de Angstrom como extenso do procedimento de cloud-screening da AERONET, study presented at the “Congresso Brasileiro de Meteorologia” (SBMET) in Florianópolis.

Reid, J. S., and P. Hobbs (1998), Physical and optical properties of young smoke from individual biomass fires in Brazil, *J. Geophys. Res.*, 103, 32, 32013-32030.

Remer, L. A., et al. (2005), The MODIS aerosol algorithm, products and validation, *J. Atmos. Sci.*, 62, 947–973.

Remer, L. A., D. Tanré, Y. J. Kaufman (2006), Algorithm for Remote Sensing of Tropospheric Aerosol from MODIS: Collection 5, Product ID: MOD04/MYD04, Algorithm Theoretical Basis Documents (ATBD's), <http://modis.gsfc.nasa.gov/data/atbd/index.php>.

Satyamurty, P., Nobre, C. and Silva Dias, P.: South America, in: *Meteorology of the Southern Hemisphere*, edited by; Karoly, D. and Vincent, D., *Meteorological Monographs*, 27(49), 119– 139, American Meteorological Society, Boston, 1998.

Seinfeld J. H. and Pandis S. N. (1998) *Atmospheric Chemistry and Physics: From Air Pollution to Climate Change*, J. Wiley, New York.

Setzer, A. and M. Pereira (1991), Amazonia biomass burnings in 1987 and an estimate of their tropospheric emissions, *Ambio*, 20, 19–22.

Twomey, S. (1977), The Influence of Pollution on the Shortwave Albedo of Clouds. *J. Atmos. Sci.*, 34, 1149–1152.

Tripathi S. N., Dey S., Chandel A., Srivastava S., Singh R. P., Holben B. N. (2005), Comparison of MODIS and AERONET derived aerosol optical depth over the Ganga Basin, India, *Annales Geophysicae*, 23, 1093-1101.

Walko R., Band L., Baron J., Kittel F., Lammers R., Lee T., Ojima D., Pielke R., Taylor C., Tague C., Tremback C., and Vidale P. (2000), Coupled Atmosphere-Biophysics-Hydrology Models for Environmental Modeling. *J. Appl. Meteorol.*, 39: (6) 931-944.

Figure Captions

Figure 1: Location of AERONET sites in South America with AOD measurements during the period 2001-2007. Map source: Google Maps

Figure 2: Typical MODIS/TERRA AOD scene at 550nm over South America on September 3, 2005

Figure 3: AOD-550nm time series (2001 - 2007) of MODIS/TERRA (black) and AERONET (red) at sites located in biomass burning influenced regions: Abracos Hill (a), Rio Branco (b), Alta Floresta (c), and Cuiabá Miranda (d). AERONET values are hourly means centered at TERRA overpass time

Figure 4: AOD-550nm time series (2001 - 2007) of MODIS/AQUA (black) and AERONET (red) at sites located in biomass burning influenced regions: Abracos Hill (a), Rio Branco (b), Alta Floresta (c), and Cuiabá Miranda (d). AERONET values are hourly means centered at AQUA overpass time

Figure 5: AOD-550nm time series (2001 - 2007) of MODIS/TERRA (black) and AERONET (red) at sites located in urban centers: São Paulo (left) and Buenos Aires (CEILAP-BA) (right). AERONET values are hourly means centered at TERRA overpass time

Figure 6: Normalized histograms of AERONET AOD bins at different sites for years 2001 - 2007, at MODIS/TERRA overpass time

Figure 7a: Correlations of MODIS/TERRA and AERONET AOD 550 nm at Alta Floresta for the burning seasons (AUG-OCT) for each year from 2001 - 2007 and integrated over the full period (bottom right). AERONET values are hourly means centered at TERRA overpass time

Figure 7b: Correlations of MODIS/AQUA and AERONET AOD 550 nm at Alta Floresta for the burning seasons (AUG-OCT) for each year from 2003 - 2007 and integrated over the full period (bottom right). AERONET values are hourly means centered at AQUA overpass time

Figure 8: Correlations of MODIS/TERRA and AERONET AOD at 550 nm integrated from 2001-2007 at all remaining AERONET sites

Figure 9: Correlations of MODIS/TERRA and AERONET AOD at 550 nm integrated from 2003-2007 at Rio Branco for MODIS-10km (a), MODIS 30-km (b) MODIS-50km (c), and MODIS 150-km (d) spatial average around the AERONET site, respectively

Figure 10: Gridded correlations of individual AERONET sites in South America data assimilation purposes, calculated by correlation studies of AERONET and MODIS/TERRA (MODIS 1 x 1) AOD at 550 nm for the burning seasons (AUG-OCT) from 2001 - 2007. Plotted AERONET sites: Abracos Hill (1), Cuiabá-Miranda (2), Rio Branco (3), Alta Floresta (4), Campo Grande Sonda (5), and Santa Cruz (8). Numbers in parentheses refer to site identification in Figure 11

Figure 11: Anisotropic radii of influence of AERONET sites in South America for data assimilation purposes, calculated by correlation studies of AERONET and MODIS (MOVAS 1° x 1°) TERRA (a) and AQUA (b) AOD at 550 nm. Plotted AERONET sites: Abracos Hill (1), Cuiabá-Miranda (2), Rio Branco (3), Alta Floresta (4), Campo Grande Sonda (5), Ceilap-BA (6), Cordoba-CETT (7), Santa Cruz (8), and São Paulo (9)

Tables:

AERONET						seasonal	max.
site	lon	lat	altitude [m]	category	data availability	mean AOD T/A	AOD
Abracos Hill	- 62.358	- 10.760	200	rural, B	2001-2005	T 0.67 ± 0.50 A 0.64 ± 0.48	2.9 2.4
Alta Floresta	- 56.017	-9.917	175	rural/urban B	2001 -2007	T 0.84 ± 0.69 A 0.80 ± 0.74	3.9 3.8
Belterra	- 54.952	-2.648	70	rural	2001 - 2003	T 0.30 ± 0.31 A 0.23 ± 0.12	2.5 0.6
Campo Grande	-	-	677	rural/urban	2003 - 2005,	T 0.39 ± 0.43	2.3
SONDA	54.538	20.438		B	2007	A 0.46 ± 0.52	3.4
CEILAP - BA	- 58.500	- 34.567	10	urban, BT	2001 - 2006	T 0.12 ± 0.14 A 0.13 ± 0.15	1.0 1.8
Cordoba -	-	-	730	urban, BT	2001 - 2007	T 0.07 ± 0.10	0.7
CETT	64.466	31.524				A 0.13 ± 0.11	0.6
Cuiabá -	-	-	210	rural, B	2001 - 2007	T 0.37 ± 0.44	3.6
Miranda	56.021	15.730				A 0.61 ± 0.62	4.7
Petrolina -	-	-9.383	370	rural	2004, 2007	T 0.11 ± 0.06	0.3
SONDA	40.500					A 0.10 ± 0.07	0.3
Rio Branco	- 67.869	-9.957	212	rural, B	2001 - 2007	T 0.65 ± 0.59 A 0.63 ± 0.64	3.9 4.2
Santa Cruz	- 63.178	- 17.802	442	urban, BT	2002, 2003, 2005	T 0.40 ± 0.43 A 0.37 ± 0.37	2.3 2.1
Santiago	- 70.717	- 33.490	510	urban	2001-2002	T 0.16 ± 0.01 A 0.16 ± 0.09	0.3 0.4
São Paulo	- 46.735	- 23.561	865	urban, BT	2001 - 2006	T 0.25 ± 0.18 A 0.31 ± 0.22	1.4 1.4

Table 1: AERONET sites description including location, altitude, categorization by urban/rural location, data availability during burning season, influence of burning

activities (B), as well as influence by transport of smoke from burning activities (BT) , mean AOD during burning season and standard deviation (T = at TERRA overpass, A = at AQUA overpass), and by maximum observed AOD concentrations

Figures:



Figure 1: Location of AERONET sites in South America with AOD measurements during the period 2001-2007. Map source: Google Maps

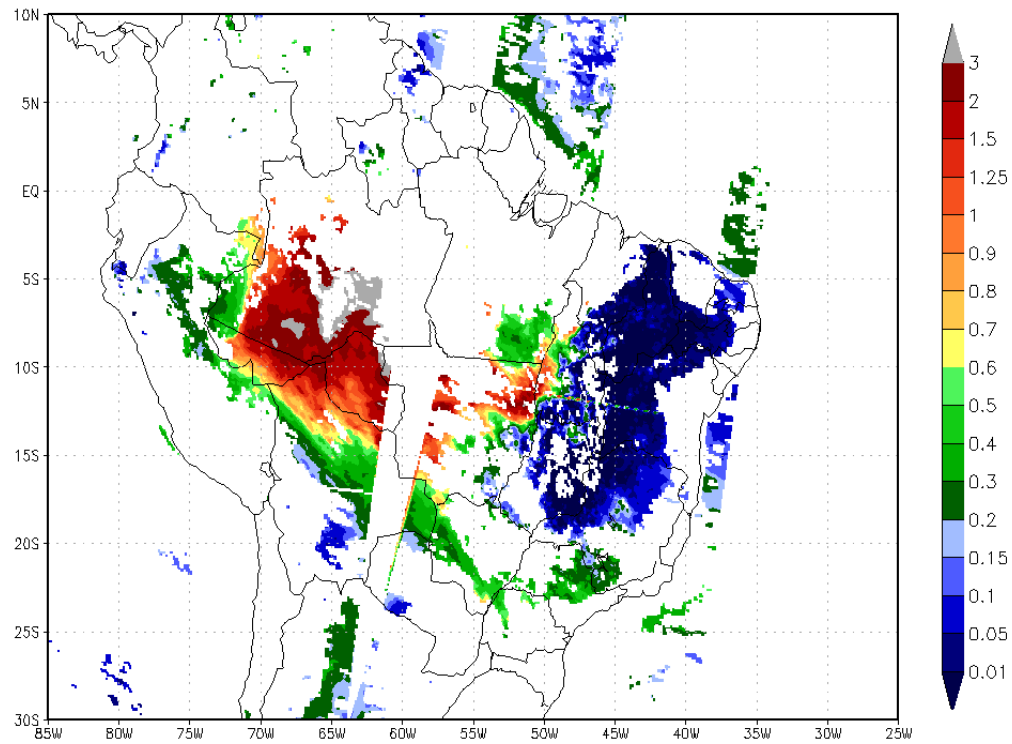


Figure 2: Typical MODIS/TERRA AOD scene at 550nm over South America on September 3, 2005

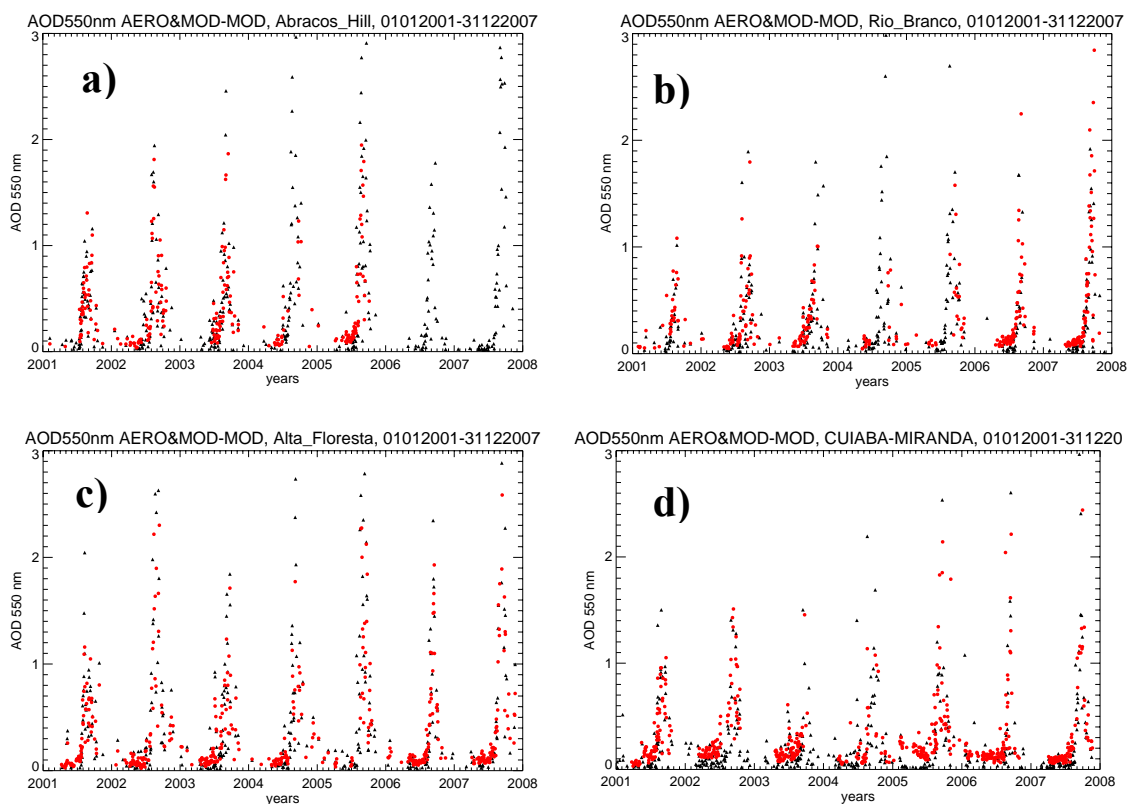


Figure 3: AOD-550nm time series (2001 - 2007) of MODIS/TERRA (black) and AERONET (red) at sites located in biomass burning influenced regions: Abracos Hill (a), Rio Branco (b), Alta Floresta (c), and Cuiabá Miranda (d). AERONET values are hourly means centered at TERRA overpass time

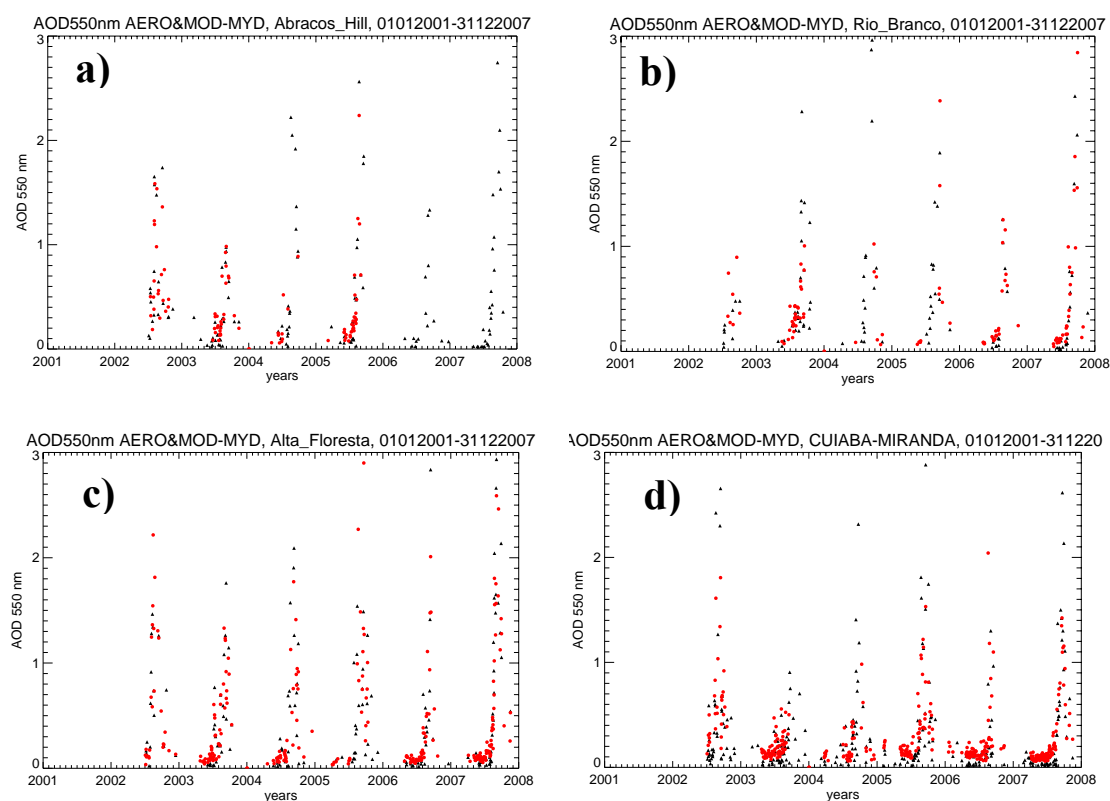


Figure 4: AOD-550nm time series (2001 - 2007) of MODIS/AQUA (black) and AERONET (red) at sites located in biomass burning influenced regions: Abracos Hill (a), Rio Branco (b), Alta Floresta (c), and Cuiabá Miranda (d). AERONET values are hourly means centered at AQUA overpass time

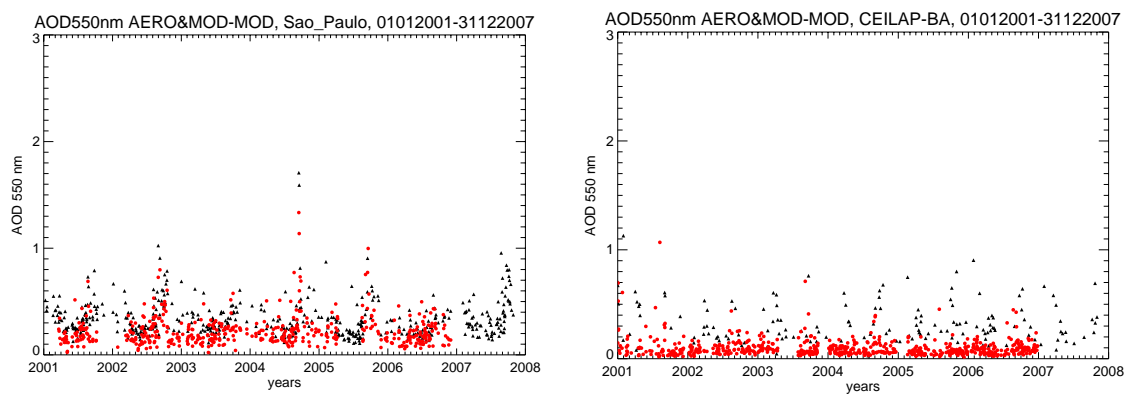


Figure 5: AOD-550nm time series (2001 - 2007) of MODIS/TERRA (black) and AERONET (red) at sites located in urban centers: São Paulo (left) and Buenos Aires (CEILAP-BA) (right). AERONET values are hourly means centered at TERRA overpass time

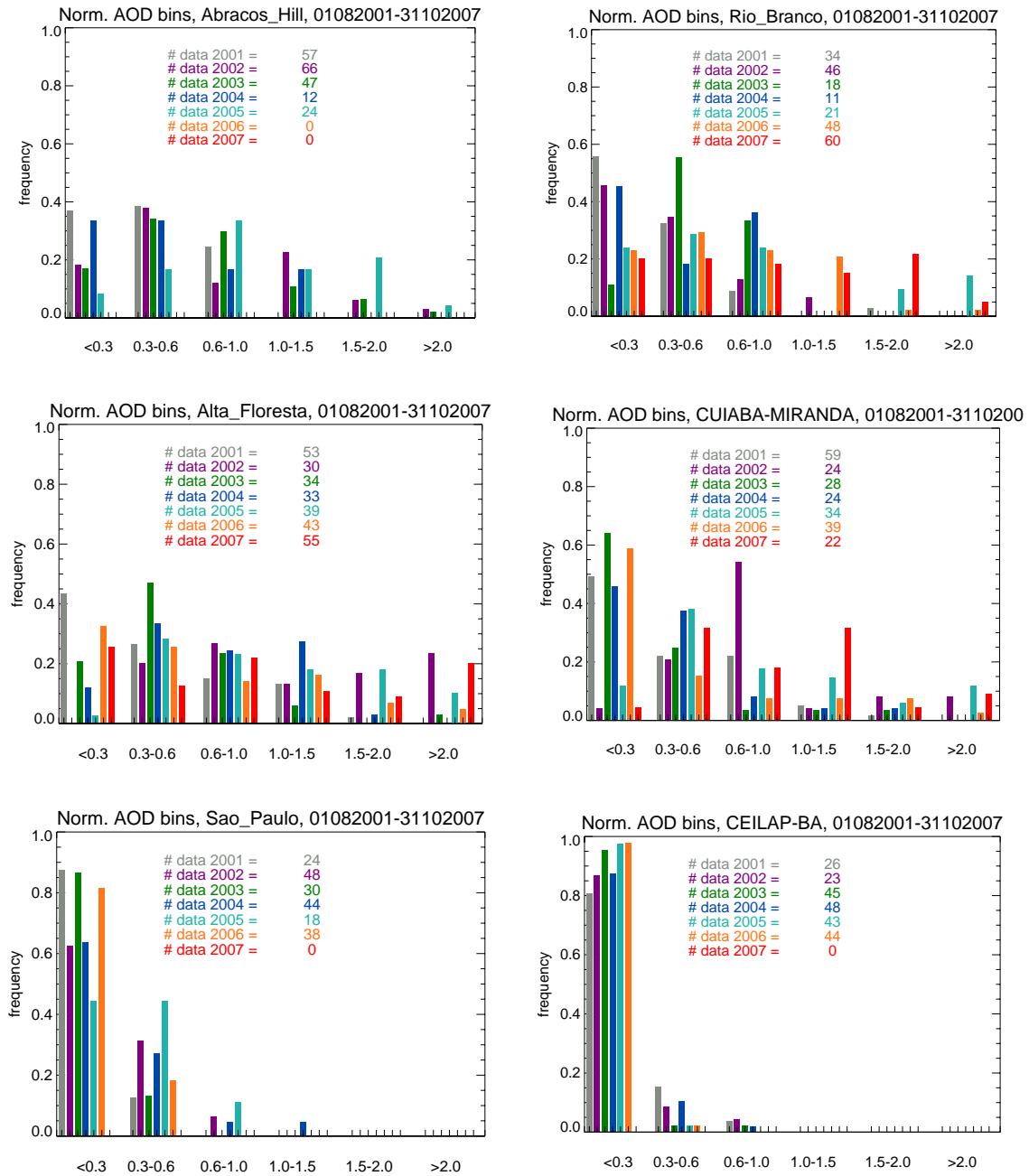


Figure 6: Normalized histograms of AERONET AOD bins at different sites for years 2001 - 2007, at MODIS/TERRA overpass time

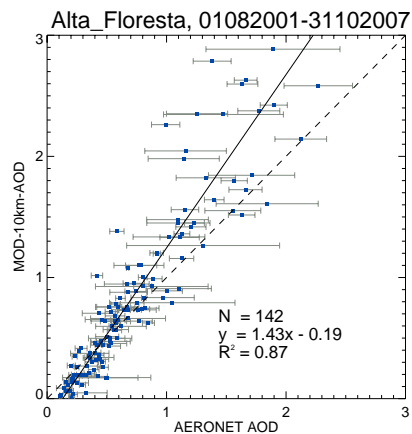
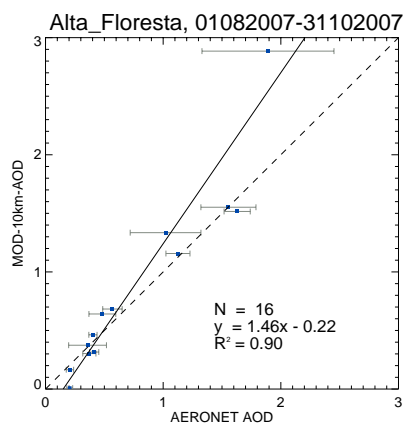
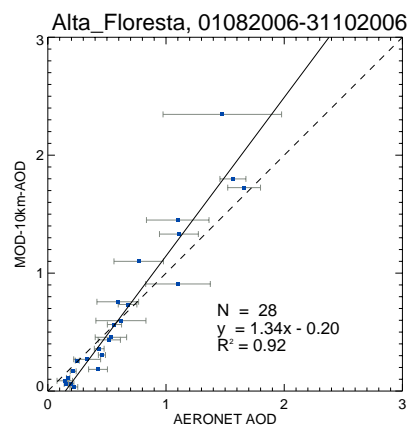
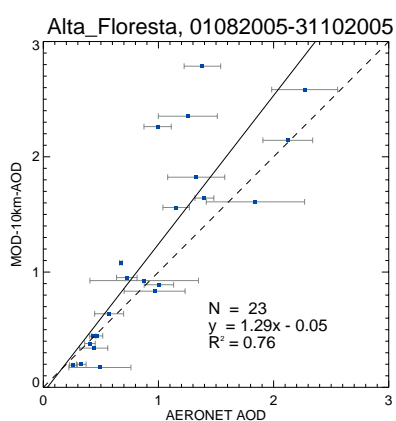
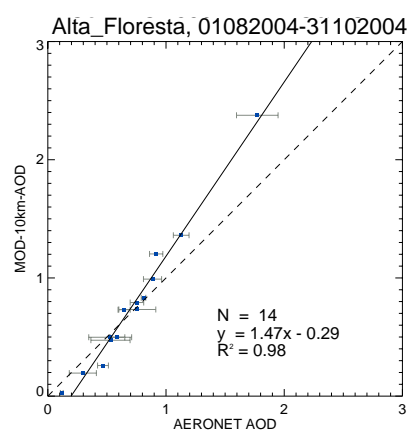
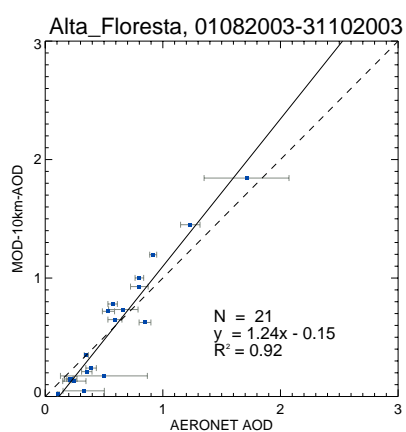
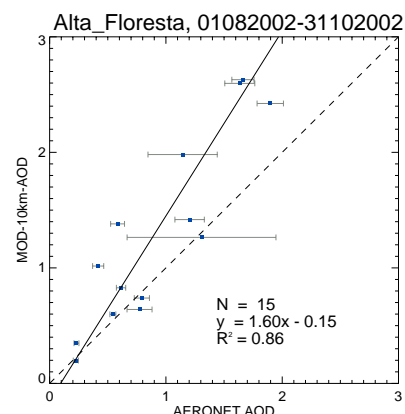
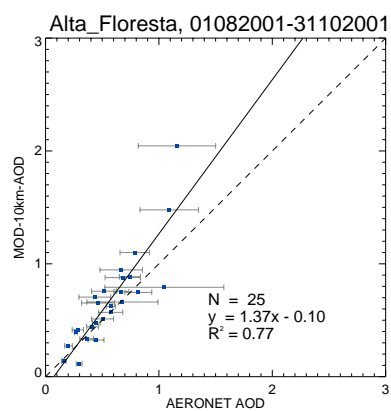


Figure 7a: Correlations of MODIS/TERRA and AERONET AOD 550 nm at Alta Floresta for the burning seasons (AUG-OCT) for each year from 2001 - 2007 and integrated over the full period (bottom right). AERONET values are hourly means centered at TERRA overpass time

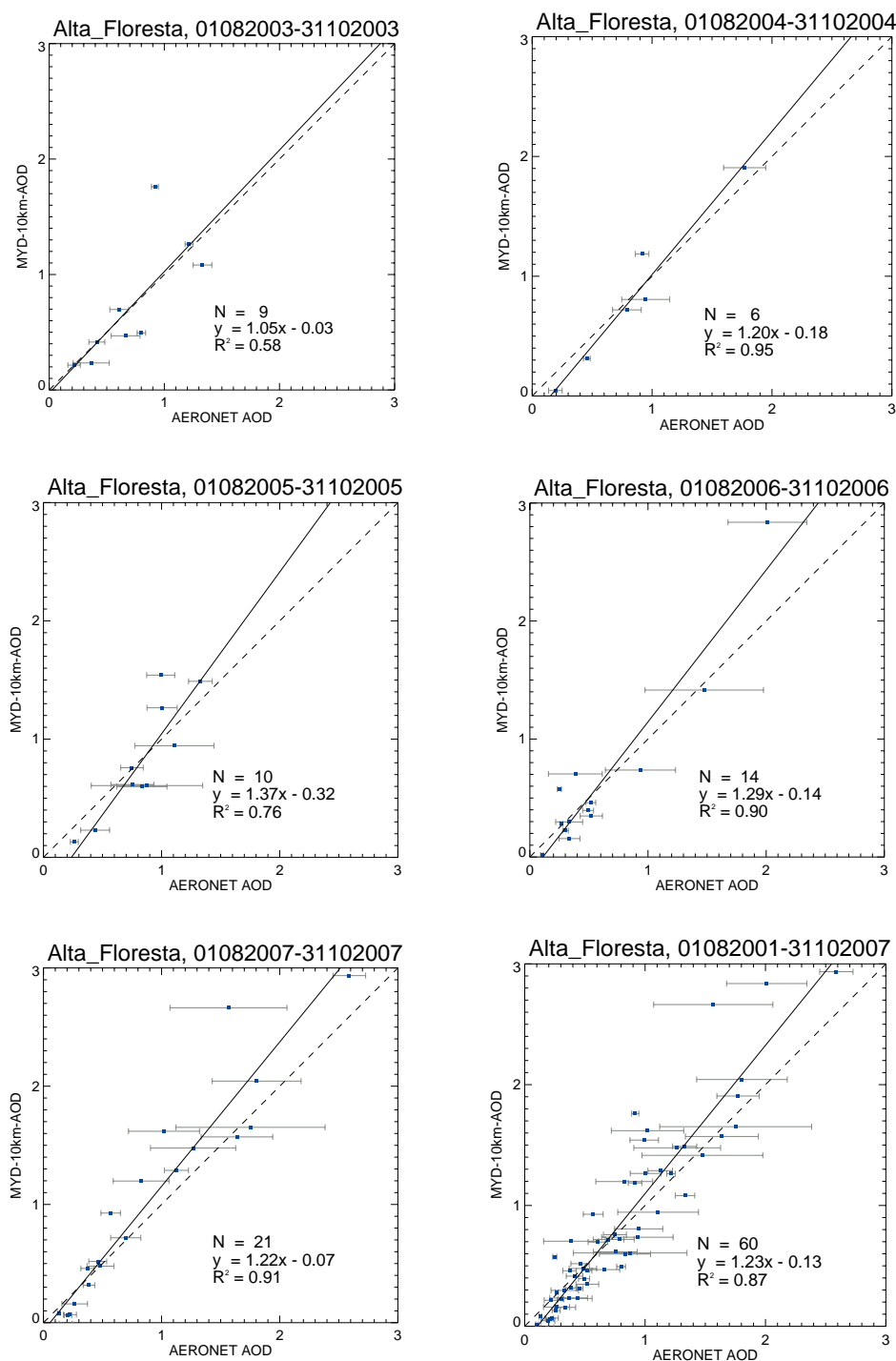


Figure 7b: Correlations of MODIS/AQUA and AERONET AOD 550 nm at Alta Floresta for the burning seasons (AUG-OCT) for each year from 2003 - 2007 and integrated over the full period (bottom right). AERONET values are hourly means centered at AQUA overpass time

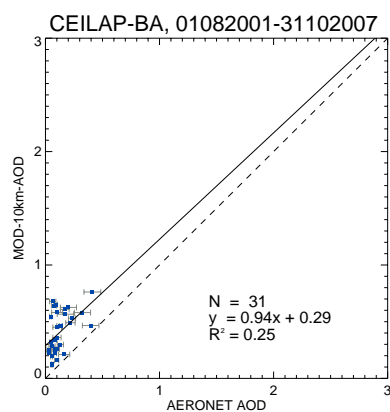
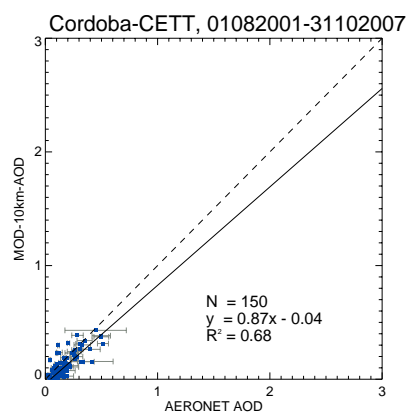
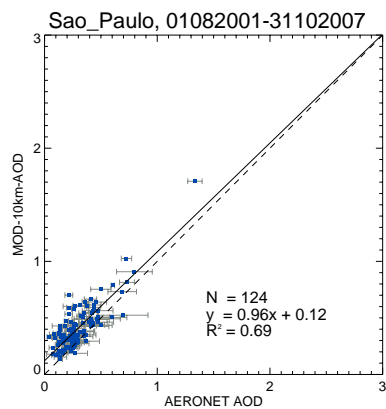
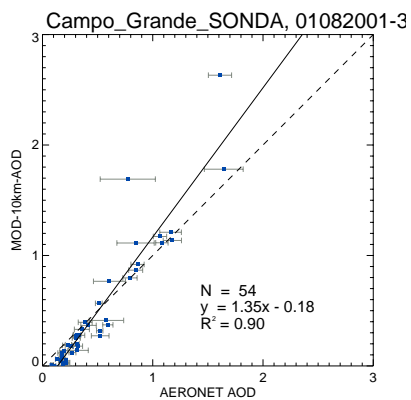
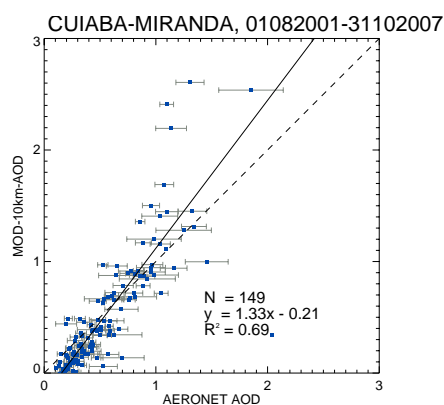
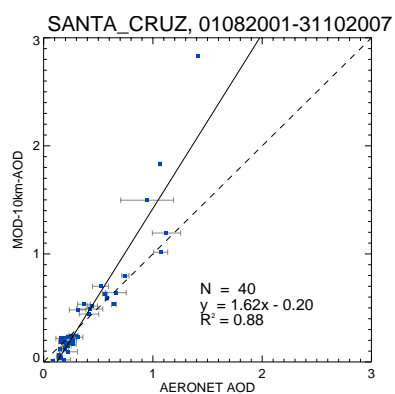
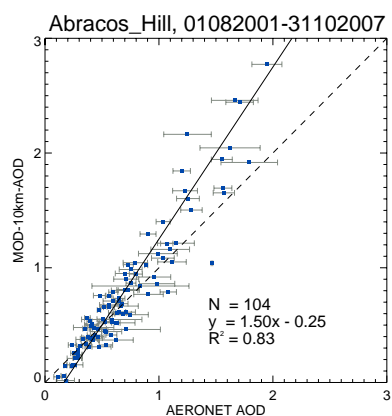
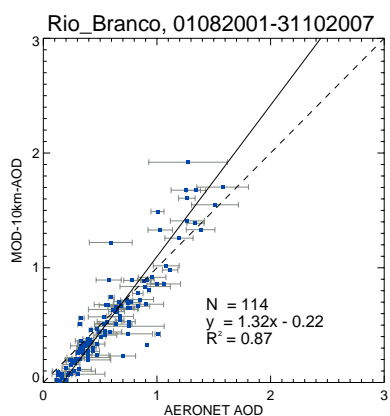


Figure 8: Correlations of MODIS/TERRA and AERONET AOD at 550 nm integrated from 2001-2007 at all remaining AERONET sites

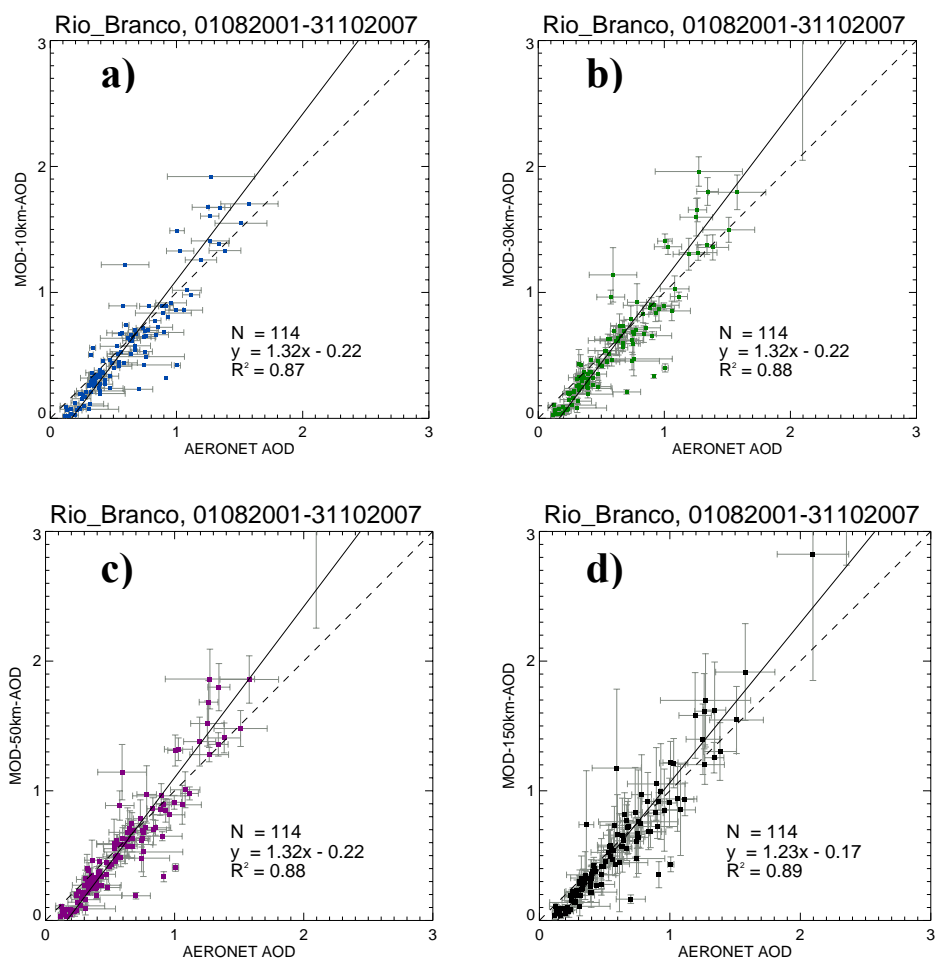


Figure 9: Correlations of MODIS/TERRA and AERONET AOD at 550 nm integrated from 2003-2007 at Rio Branco for MODIS-10km (a), MODIS 30-km (b) MODIS-50km (c), and MODIS 150-km (d) spatial average around the AERONET site, respectively

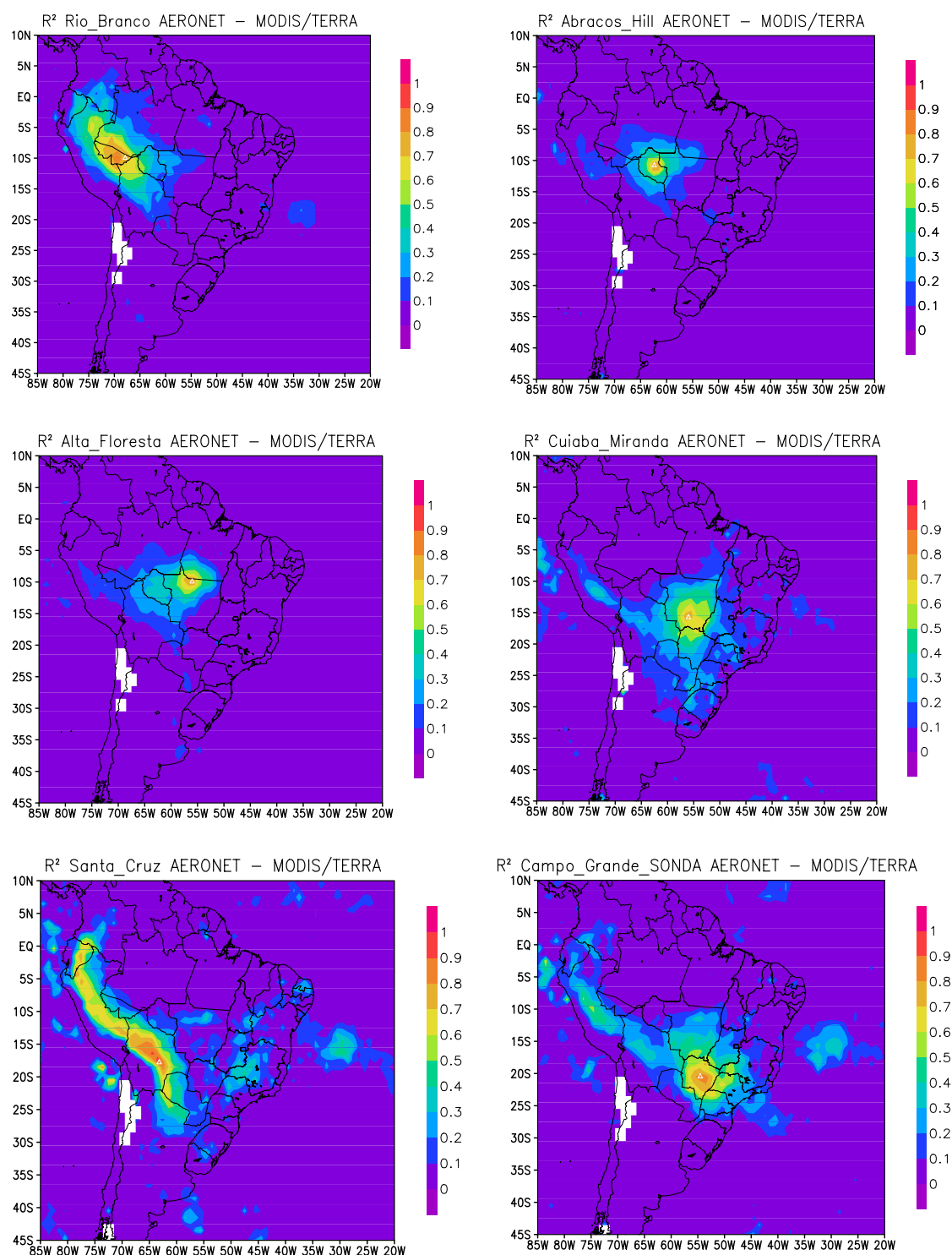


Figure 10: Gridded correlations of individual AERONET sites in South America data assimilation purposes, calculated by correlation studies of AERONET and MODIS/TERRA (MOVAS 1 x 1) AOD at 550 nm for the burning seasons (AUG-OCT) from 2001 - 2007. Plotted AERONET sites: Abracos Hill (1), Cuiabá-Miranda (2), Rio

Branco (3), Alta Floresta (4), Campo Grande Sonda (5), and Santa Cruz (8). Numbers in parentheses refer to site identification in Figure 11

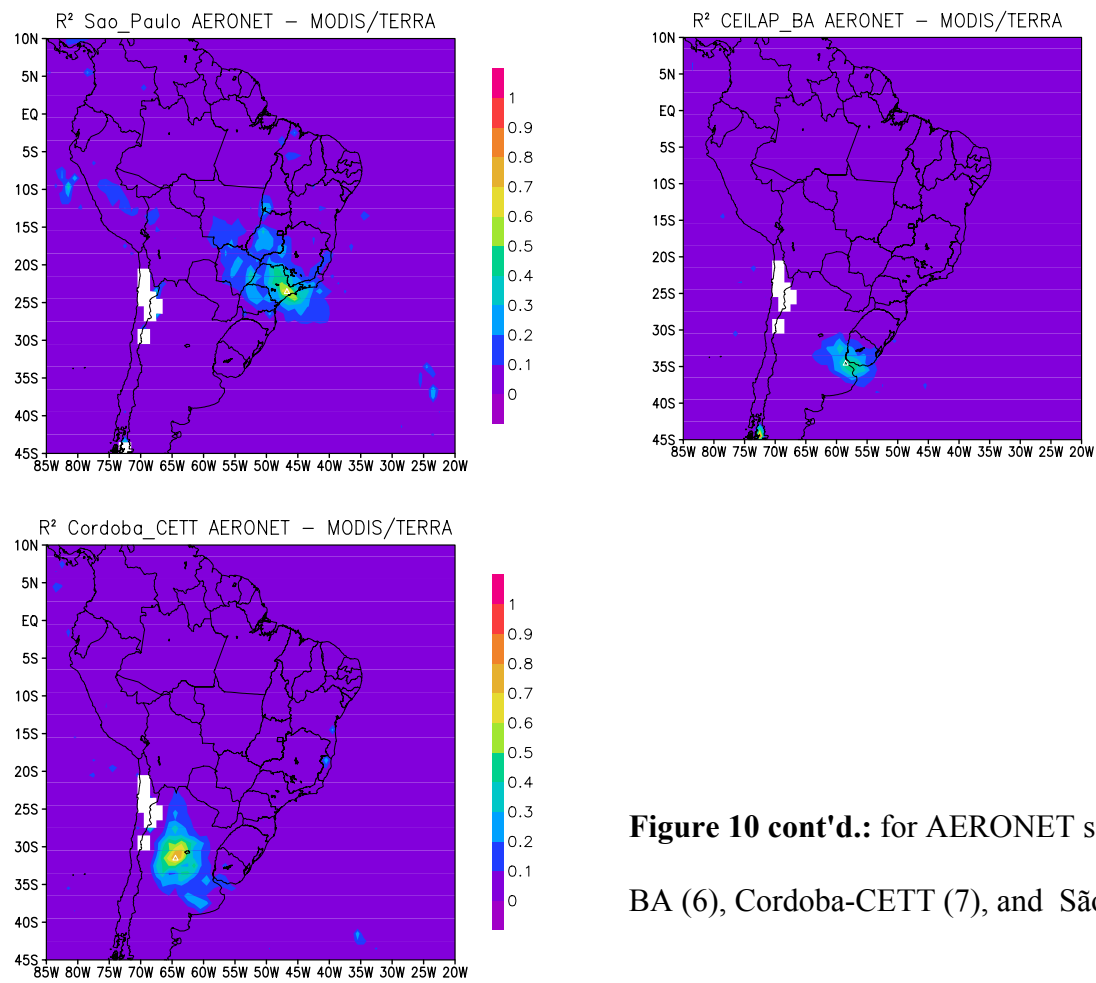
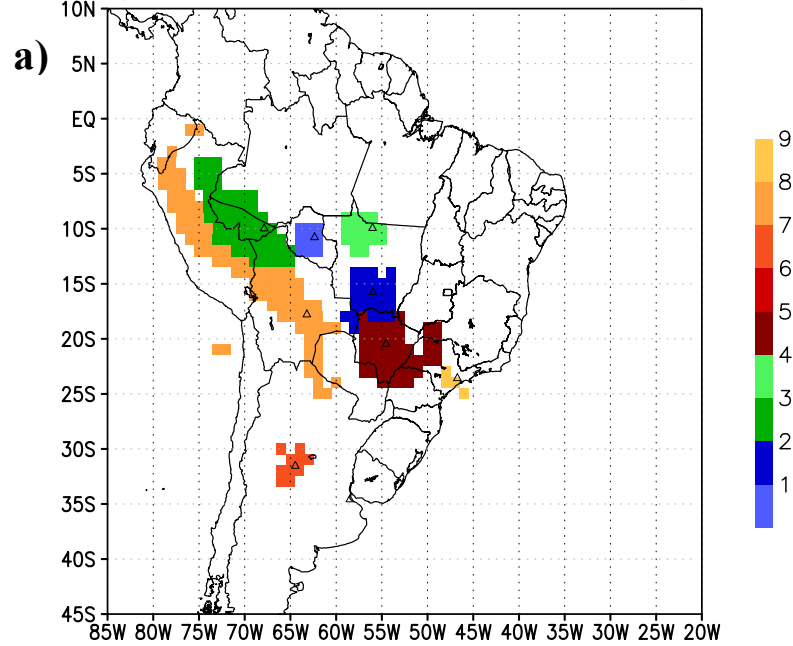


Figure 10 cont'd.: for AERONET sites Ceilap-BA (6), Cordoba-CETT (7), and São Paulo (9)

Anisotropic radii of influence AERONET – MODIS/TERRA



Anisotropic radii of influence AERONET – MODIS/AQUA

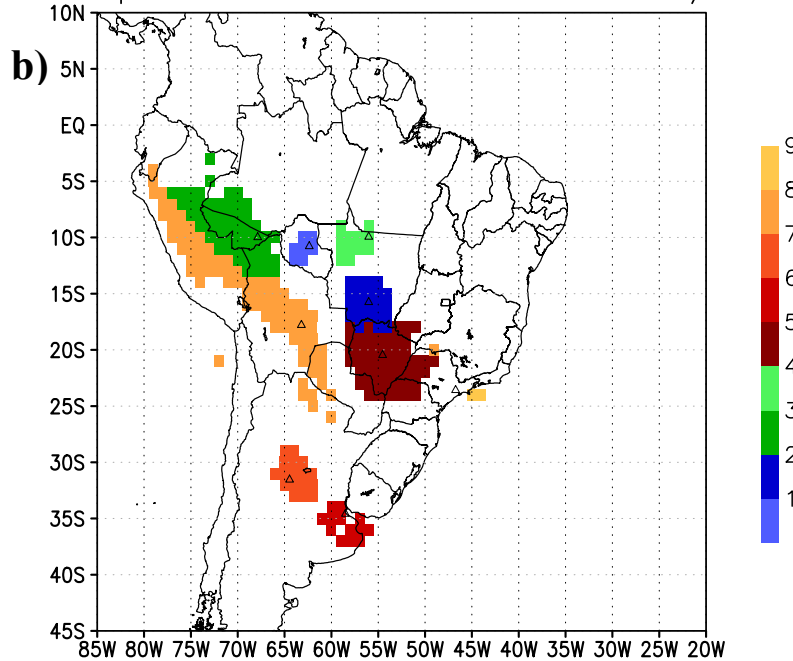


Figure 11: Anisotropic radii of influence of AERONET sites in South America for data assimilation purposes, calculated by correlation studies of AERONET and MODIS (MOVAS 1°x1°) TERRA (a) and AQUA (b) AOD at 550 nm. Plotted AERONET sites: Abracos Hill (1), Cuiabá-Miranda (2), Rio Branco (3), Alta Floresta (4), Campo Grande Sonda (5), Ceilap-BA (6), Cordoba-CETT (7), Santa Cruz (8), and São Paulo (9)